Generating Susceptibility Weighted Images using susceptibility maps

Karen Mok[1], Jaladhar Neelavalli[2], Saifeng Liu[3], and E. Mark Haacke[4,5]

[1]Mcmaster University, Hamilton, ON, Canada, [2]Department of Radiology, Wayne State University, [3]McMaster University, [4]Wayne State University, [5]School of Biomedical Engineering, McMaster University

Introduction: SWI is a widely used clinical tool for venography in the brain [1]. It is a unique imaging methodology which combines the magnitude and phase information, where phase is assumed to be directly related or proportional to the magnetic susceptibility of the structure. While this is true, the actual phase effects are dependent on tissue orientation, as well as the size and shape of the vessels and paramagnetic structures inside the brain. The phase images are also affected by local and global susceptibility effects arising from tissue interfaces between air and bone. At typical imaging resolutions of high in-plane and low through-plane resolution (i.e. voxel aspect ratios from in-plane to slice direction varying from 1:2 to 1:5), due to phase integration effects, the sign of the venous vessel phase turns out to be quite robustly consistent, independent of the vessel orientation. This is partly the reason why SWI typically acquired axially is so successful in depicting the veins exquisitely. However, at isotropic resolutions, when there are minimal phase integration effects, veins have different signs in the phase images depending on their orientation. This creates a problem in generating a proper phase based mask for susceptibility weighting. There have been attempts to use bi-directional masks which use both positive and negative signed phase values in their mask creation [2]. Although this may provide good venograms, it can also lead to artifacts due to remnant phase wraps. In this abstract, we evaluate the possibility of using the susceptibility map, instead of phase, to create the mask for susceptibility weighting. Since susceptibility maps are orientation independent, they provide more accurate representation of the brain as well as reducing the enlargement effect of the vessels in the brain due dipole effects.

Method: *In vivo* datasets of two healthy volunteers were collected using 3D gradient echo sequences both with 0.5mm isotropic resolution at 3T. For the first dataset, the following parameters were used: TR 24ms, TE 17ms, FA 15°, BW 181 Hz/pixel, matrix size 512x368x224. For the second dataset: TR 26ms, TE 17.3ms, FA 15°, BW 121 Hz/pixel, matrix size 512x368x 256. Anisotropic datasets with 0.5x0.5x2 mm^3 resolution were obtained from these datasets by complex averaging. The upper region of the brain was processed using the isotropic data, where 64 slices from the midbrain to the cortex were visualized. QSM images were generated using a regularized inverse filtering procedure as described in [3], with a kspace truncation value of 0.1. Before the inverse filtering, skull-stripping and zero-padding to the matrix size 512 x 512 x 128 were performed using customized software. A series of masks were generated using the susceptibility maps with a dual-threshold method: w=[(Th1 - χ) /(Th1 − Th2)]^n. The pixels with susceptibility values above the upper threshold, Th1, were set to 0 in the masks and were set to 1 if the susceptibility values were below the lower threshold value, Th2. The following parameters were processed by varying each of the three parameters, Th1, Th2, and *n*: Th 1 = 5000, 1000, 800, 600, 400; Th2 = 120, 100, 80, 25, 15, 0. *n* = 3, 4, 5. These masks were multiplied to the original magnitude images to construct the tSWI images, and the minimal intensity projection (mIP) were generated for comparison. After processing a total of 4 isotropic and anisotropic datasets, visual inspection and magnitude profiling using Matlab and customized software was performed across different vessels, namely the large thalamostriate vein and the small vessel on the central sulcus on the right side of the brain. Slice-by-slice comparison with SWI images and mIPs of the SWI images were used to determine optimal Th1, Th2 and n parameters.

Table 1: The maximum threshold (Th1), the minimum threshold (Th2), and the number of vessel map multiplications (n) in the 4 datasets. A1: anisotropic dataset 1, A2: anisotropic dataset 2, I1: isotropic dataset 1, I2: isotropic dataset 2

	A1	A2	I1	I2
Th1 (ppb)	800	1000, 800	1000	800
Th2 (ppb)	0	0	0	0
n	4	4	4	3

Results: The final threshold values are shown in **Table 1**. The threshold of susceptibility values were within the range 1000 and 800ppb for both isotropic and anisotropic datasets, with the optimal lower threshold being Th2 = 0. The value of n= 4 was optimal for most cases for deep grey matter structures visualization and grey matter/white matter contrast. A comparison between the original magnitude image, the SWI image and the tSWI image of the isotropic data is provided in Figure 2, together with the high-pass filtered phase image (with filter size 64x64) and the corresponding susceptibility map. As pointed by the white arrows, the sign of the phase of the vein varies spatially due to the orientation of the vein. This vein has inconsistent intensity and may not be visible in the final SWI image. However it is properly visualized by the tSWI image. The datasets were compared by mIPping every 8 slices, with a sliding window of 4 (Figure 3). tSWI images are shown not only lead to better visualization of the veins, but also a better contrast-to-noise ratio of gray matter structures.

In Figure 2, showing isotropic data, demonstrates the through-plane resolution effect in SWI images, where vessels perpendicular to the main field will have differing phase intensities corresponding to different vessel orientation (Fig 2b). Fig 2c shows the generated susceptibility map which shows the full vessel, while Fig 2c shows a vessel with more continuous intensity compared with SWI (Fig 2d). This is also observed in the central veins on this same slice.

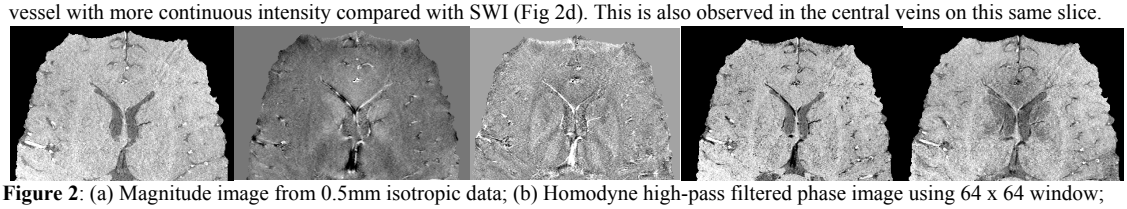

Figure 2: (a) Magnitude image from 0.5mm isotropic data; (b) Homodyne high-pass filtered phase image using 64 x 64 window; (c) susceptibility map of isotropic data using threshold value of 0.1; (d) tSWI image after vessel map multiplication of 3; (d) conventional SWI image from 64 sized Homodyne filtered phase vessel mask.

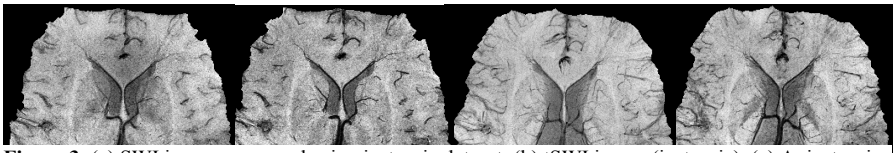

Figure 3: (a) SWI image processed using isotropic dataset; (b) tSWI image (isotropic). (c) Anisotropic conventional SWI image; (d) anisotropic tSWI image. Note the thalamostriate veins are more prominent using tSWI and inhomogeneities are reduced compared to conventional SWI. Vessels can be seen more prominently.

Discussion and Conclusion: tSWI allows the SWI procedure to be used for isotropic datasets and allows for increasingly robust visualization of vessels and grey matter structures within the brain. It also has higher CNR and thus, can more easily view abnormalities in vasculatures. Using a simple dual-threshold approach, sufficient vessel maps can be obtained to produce orientation independent SWI images. Unlike the traditional SWI which uses relatively stable processing parameters, the contrast in tSWI images depend on the selection of the two thresholds. In choosing the vessel mask parameters, larger vessels with a high susceptibility would intensify quicker with increasing value of *n*, while smaller vessels would intensify at a slower rate. A balance between keep large vessels under saturation while amplifying the small vessels sufficiently is required. Although optimal values for the vessel mask has been found, a possible method for rectifying this is through the iterative SWIM approach[4], which reduces streaking artifacts of the QSMs while also causing increased susceptibility values and improving tSWI quality. ***References***: [1] Mittal. et al. AJNR, 2009; [2] Haacke et al. "Susceptibility weighted imaging in MRI". Wiley, 2010; [3] Haacke et al. JMRI, 2010; [4] Tang. et al, ISMRM 2011:4476